

tion, we mutated this position in the PGT minigene. As seen in Fig. 4B (lanes 4 and 5), this point mutation was enough to activate the nearly constitutive inclusion of the *Alu* exon in the mature transcript. As indicated above, the same mutation in the COL4A3 gene activates a constitutive exonization of a silent intronic *Alu*, resulting in Alport syndrome (10). To assess the importance of our findings, we analyzed the entire content of *Alus* in the human genome and found that there are at least 238,000 antisense *Alus* located within introns in the human genome (20). Of these, 52,935 *Alus* carry a potential ADAR2-like 3'SS, and 23,012 carry a potential PGT-like 3'SS. Our results suggest that many of these silent intronic *Alu* elements might be susceptible to exonization by the same single point mutation and are thus under strict selective pressure. Such point mutations in human genomic antisense *Alus* may, therefore, be the molecular basis for predisposition to so-far uncharacterized genetic diseases.

Because all *Alu*-containing exons are alternatively spliced (9), they add splice variants to our transcriptome while maintaining the original proteins intact. Exonized *Alus* can, thus, acquire functionality and become exapted, i.e., adapted to a function different than their original (21). When the splicing of an *Alu* exon is constitutive, however, the transcript encoding to the original protein is permanently disrupted, which could provide the basis for a genetic disorder. Identification of genomic *Alus* that are one point mutation away from exonization might therefore enable the screening for predisposition to genetic diseases that involve *Alu* exonization.

References and Notes

1. A. J. Mighell, A. F. Markham, P. A. Robinson, *FEBS Lett.* **417**, 1 (1997).
2. D. J. Rowold, R. J. Herrera, *Genetica* **108**, 57 (2000).
3. C. W. Schmid, *Prog. Nucleic Acid Res. Mol. Biol.* **53**, 283 (1996).
4. E. S. Lander et al., *Nature* **409**, 860 (2001).
5. A. M. Roy-Engel et al., *Genome Res.* **12**, 1333 (2002).
6. W. Makalowski, G. A. Mitchell, D. Labuda, *Trends Genet.* **10**, 188 (1994).
7. W. Makalowski, *Gene* **259**, 61 (2000).
8. A. Nekrutenko, W. H. Li, *Trends Genet.* **17**, 619 (2001).
9. R. Sorek, G. Ast, D. Graur, *Genome Res.* **12**, 1060 (2002).
10. B. Knebelmann et al., *Hum. Mol. Genet.* **4**, 675 (1995).
11. G. A. Mitchell et al., *Proc. Natl. Acad. Sci. U.S.A.* **88**, 815 (1991).
12. R. Vervoort, R. Gitzelmann, W. Lissens, I. Liebaers, *Hum. Genet.* **103**, 686 (1998).
13. K. Chua, R. Reed, *Nature* **402**, 207 (1999).
14. K. Chua, R. Reed, *Mol. Cell. Biol.* **21**, 1509 (2001).
15. R. E. Manrow, S. L. Berger, *J. Mol. Biol.* **234**, 281 (1993).
16. D. Slavov, K. Gardiner, *Gene* **299**, 83 (2002).
17. F. Lai, C. X. Chen, K. C. Carter, K. Nishikura, *Mol. Cell. Biol.* **17**, 2413 (1997).
18. Materials and methods are available as supporting material on Science Online.
19. G. Lev-Maor, R. Sorek, N. Shomron, G. Ast, unpublished data.
20. R. Sorek, R. Shalgi, G. Ast, D. Graur, unpublished data.
21. J. Brosius, S. J. Gould, *Proc. Natl. Acad. Sci. U.S.A.* **89**, 10706 (1992).
22. M. Mihovilovic et al., *Biochem. Biophys. Res. Commun.* **197**, 137 (1993).
23. M. Miller, K. Zeller, *Gene* **190**, 309 (1997).

24. W. G. Cance, R. J. Craven, T. M. Weiner, E. T. Liu, *Int. J. Cancer* **54**, 571 (1993).
25. I. W. Caras et al., *Nature* **325**, 545 (1987).
26. G. Svineng, R. Fassler, S. Johansson, *Biochem. J.* **330**, 1255 (1998).
27. J. Jurka, A. Milosavljevic, *J. Mol. Evol.* **32**, 105 (1991).
28. RepeatMasker is available online at <http://repeatmasker.genome.washington.edu/cgi-bin/RepeatMasker>.
29. We thank M. Kupiec for a critical reading; R. Reed for the hSlu7 plasmid; and also F. Belinky, R. Shalgi, T. Dagan, and E. Sharon for assistance in *Alu* data analysis. Supported by a grant from the Israel Science

Foundation and, in part, by a grant from the Israel Cancer Association and the Indian-Israeli Scientific Research Corporation to G.A.

**Supporting Online Material**  
[www.sciencemag.org/cgi/content/full/300/5623/1288/DC1](http://www.sciencemag.org/cgi/content/full/300/5623/1288/DC1)  
 Materials and Methods  
 Fig. S1  
 Table S1  
 References and Notes

21 January 2003; accepted 9 April 2003

## Essential Role of Fkbp6 in Male Fertility and Homologous Chromosome Pairing in Meiosis

Michael A. Crackower,<sup>1\*</sup> Nadine K. Kolas,<sup>2\*</sup> Junko Noguchi,<sup>4</sup> Renu Sarao,<sup>1</sup> Kazuhiro Kikuchi,<sup>4</sup> Hiroyuki Kaneko,<sup>4</sup> Eiji Kobayashi,<sup>5</sup> Yasuhiro Kawai,<sup>6</sup> Ivona Kozieradzki,<sup>1</sup> Rushin Landers,<sup>1</sup> Rong Mo,<sup>7</sup> Chi-Chung Hui,<sup>7</sup> Edward Nieves,<sup>3</sup> Paula E. Cohen,<sup>2</sup> Lucy R. Osborne,<sup>8</sup> Teiji Wada,<sup>1</sup> Tetsuo Kunieda,<sup>6</sup> Peter B. Moens,<sup>9</sup> Josef M. Penninger<sup>1†</sup>

Meiosis is a critical stage of gametogenesis in which alignment and synapsis of chromosomal pairs occur, allowing for the recombination of maternal and paternal genomes. Here we show that FK506 binding protein (Fkbp6) localizes to meiotic chromosome cores and regions of homologous chromosome synapsis. Targeted inactivation of *Fkbp6* in mice results in aspermic males and the absence of normal pachytene spermatocytes. Moreover, we identified the deletion of *Fkbp6* exon 8 as the causative mutation in spontaneously male sterile *as/as* mutant rats. Loss of Fkbp6 results in abnormal pairing and misalignments between homologous chromosomes, nonhomologous partner switches, and autosynapsis of X chromosome cores in meiotic spermatocytes. Fertility and meiosis are normal in *Fkbp6* mutant females. Thus, Fkbp6 is a component of the synaptonemal complex essential for sex-specific fertility and for the fidelity of homologous chromosome pairing in meiosis.

Meiosis is a fundamental process in sexually reproducing species that allows genetic exchange between maternal and paternal ge-

nomes (1, 2). Defects in high-fidelity meiotic chromosome alignment or in genome segregation in germ cells result in aneuploidies such as trisomy 21 in Down syndrome. Aneuploidy is a leading cause of spontaneous miscarriage in humans and a hallmark of many human cancer cells (2). Once homologs are paired, the chromosomes are connected by a specific structure: the synaptonemal complex (SC) (3). SCs are zipperlike structures assembled along the paired meiotic chromosomes during the prophase of the first meiotic division (3). Although SCs were first discovered more than 45 years ago (4, 5), only very few structural meiosis-specific components of the SC have been identified in mammals, such as SC proteins 1, 2, and 3 [Scp1 (also known as Syn1/Sycp1), Scp2, and Scp3 (also known as Cor1)] (3). Genetic inactivation of the mouse *Scp3* gene results in male infertility due to a failure to form chromosome synapsis in meiotic prophase (6). Female *Scp3*<sup>-/-</sup> mice have reduced fertility, and embryos from *Scp3*<sup>-/-</sup> mothers have increased incidents of aneuploidy (7). To our

<sup>1</sup>Institute of Molecular Biotechnology of the Austrian Academy of Sciences (IMBA), c/o Dr. Bohrgasse 7, 1030, Vienna, Austria. <sup>2</sup>Department of Molecular Genetics, and <sup>3</sup>Department of Biochemistry, Laboratory for Macromolecular Analysis and Proteomics, Albert Einstein College of Medicine (AECOM), 1300 Morris Park Avenue, Bronx, NY 10461, USA. <sup>4</sup>Germ Cell Conservation Laboratory, National Institute of Agrobiological Sciences, Kannondai, Tsukuba, Ibaraki 305-8602, Japan. <sup>5</sup>National Livestock Breeding Center, Odakura, Nishigo, Fukushima 961-851, Japan. <sup>6</sup>Graduate School of Natural Science and Technology, Okayama University, Okayama 700-0082 Japan. <sup>7</sup>Program in Developmental Biology, The Hospital for Sick Children, Toronto, ON M5G 1X8, Canada. <sup>8</sup>Departments of Medicine and Molecular and Medical Genetics, University of Toronto, 1 King's College Circle, Toronto, ON M5S 1A8, Canada. <sup>9</sup>Department of Biology, York University, Toronto, ON M3J 1P3, Canada.

\*These authors contributed equally to this work.  
 †Present address: Department of Protein Sciences, Amgen, Thousand Oaks, CA 91320, USA.  
 ‡To whom correspondence should be addressed. E-mail: josef.penninger@oeaw.ac.at

## REPORTS

knowledge, genetic inactivation of *Scp1* or *Scp2* has not been reported yet.

FK506 binding protein 6 (*Fkbp6*) is a member of a gene family that contains a prolyl isomerase/FK506 binding domain and tetratricopeptide protein-protein interaction domains (8). *Fkbp6* maps to human chromosome 7q11.23 and is commonly deleted in Williams-Beuren syndrome (8), an autosomal, dominant, contiguous gene deletion disorder that encompasses at least 17 different genes and is characterized by a diverse array of abnormalities (9). Here we show that *Fkbp6* is an SC component essential for sex-specific fertility and for the fidelity of homologous chromosome pairing in meiosis.

To study the role of *Fkbp6* in vivo, we cloned the mouse *Fkbp6* homolog by reverse transcription–polymerase chain reaction (RT-PCR) from mouse testis RNA (fig. S1). Mouse *Fkbp6* mRNA expression was restricted to the testes (Fig. 1A). *Fkbp6* mRNA (fig. S1B) and protein (Fig. 1B) were found in the cytoplasm and nucleus of spermatocytes. *Fkbp6* was lost as cells exited prophase I and was not detected in spermatids. In meiotic chromosome spreads, *Fkbp6* protein was weakly associated with the chromosome cores before synapsis and SC formation at early prophase (Fig. 1, C and D). At the pachytene stage, in which SCs are fully as-

sembled, *Fkbp6* was strongly localized to the SC (Fig. 1, E and F). At the diplotene (late meiotic prophase) stage, in which the homologous chromosomes have initiated repulsion while remaining synapsed, *Fkbp6* expression in the chromosome cores was markedly reduced (Fig. 1, G and H). *Fkbp6* was also present at the male-specific double dense body (DDB) associated with the X-chromosome core (Fig. 1E). Moreover, at the pachytene and diplotene stages, *Fkbp6* colocalized with *Scp3* at the synapsed regions of autosomal chromosomes (fig. S2, A to D). As in male germ cells, *Fkbp6* was strongly expressed at the synapsed cores during mid-prophase in female meiotic cells, and *Fkbp6* expression declined thereafter (fig. S2, E to H). We detected *Fkbp6* expression within the SC using immunogold labeling and electron microscopy (EM) of individual prophase chromosomes (Fig. 1I) (10). Thus, *Fkbp6* is an SC component.

To determine the functional role of *Fkbp6* in vivo, we generated mice deficient for *Fkbp6* (fig. S3). Both male and female *Fkbp6*-mutant mice are healthy and have normal life-spans. Extensive analysis showed that no other abnormalities could be detected in any tissues of male *Fkbp6*-deficient mice. Male, but not female, mice deficient for *Fkbp6* were completely sterile. Testes of all

*Fkbp6*<sup>-/-</sup> males were reduced in size (Fig. 2A). The testis size and fertility of *Fkbp6*<sup>+/-</sup> mice resembled that of wild-type littermates. Histological analysis revealed that *Fkbp6*<sup>-/-</sup> male mice lacked spermatids, and we did not observe any mature spermatozoa in the caudal epididymis or seminiferous tubules (Fig. 2, B and C). Loss of *Fkbp6* expression resulted in abnormal pachytene spermatocytes, defined by the appearance of unusual inclusion bodies and dense compacted nuclei; spermatocytes failed to proceed beyond the pachytene stage (Fig. 2, D and E). No alterations in testosterone, luteinizing hormone, follicle-stimulating hormone, or estradiol were detected, indicating that hormonal imbalances do not contribute to the phenotype. Staining by terminal deoxynucleotidyl transferase-mediated deoxyuridine triphosphate nick end labeling (TUNEL) revealed an increase in apoptosis in spermatocytes of mutant mice (fig. S4, A to D). This increase in cell death was most prevalent at 21 days after birth (fig. S4, C and D), indicating the presence of the spermatogenic defect during the first wave of meiosis in pubescent animals. Mitotic proliferation of progenitor spermatogonia appeared to proceed normally in *Fkbp6*<sup>-/-</sup> testes (fig. S4, E and F). Defective spermatogenesis and the complete absence of spermatids and spermatozoa in *Fkbp6*<sup>-/-</sup> males was confirmed with EM (Fig. 2, F and G). The presence of Sertoli cells in the seminiferous tubules suggests that the intratubular environment was normal. Thus, loss of *Fkbp6* results in male-specific infertility due to a complete block in spermatogenesis and cell death of meiotic spermatocytes.

Various natural aspermic rat and mouse mutants have been described (11, 12). The overall histological phenotypes of natural mutant, aspermic *as/as* rats are very similar to that observed in our *Fkbp6*<sup>-/-</sup> mice, including the presence of the inclusion bodies in spermatocytes (12–14) and apparently abnormal spermatocyte chromosomes (15). The *as/as* phenotype is controlled by an autosomal recessive allele that maps to rat chromosome 12 in a region syntenic to the human Williams-Beuren critical region (14, 15). Therefore, a mutation in the rat *Fkbp6* gene may be the causative mutation of *as/as* rats.

We amplified the entire *Fkbp6* coding region from normal and *as/as* rats. The 3' *Fkbp6* gene region in the mutant *as/as* rats was shorter than that of wild types (Fig. 3A). Comparison of the nucleotide sequence revealed that a 93–base pair (bp) region corresponding to exon 8 of the gene was deleted in the mutant rats (Fig. 3B). Fine mapping showed that *as/as* rats harbored a genomic deletion of a 9357-bp region that includes exon 8 of the *Fkbp6* gene (fig. S5). Genomic deletion of exon 8 resulted in *Fkbp6* protein expression from *as/as* testes that was unde-

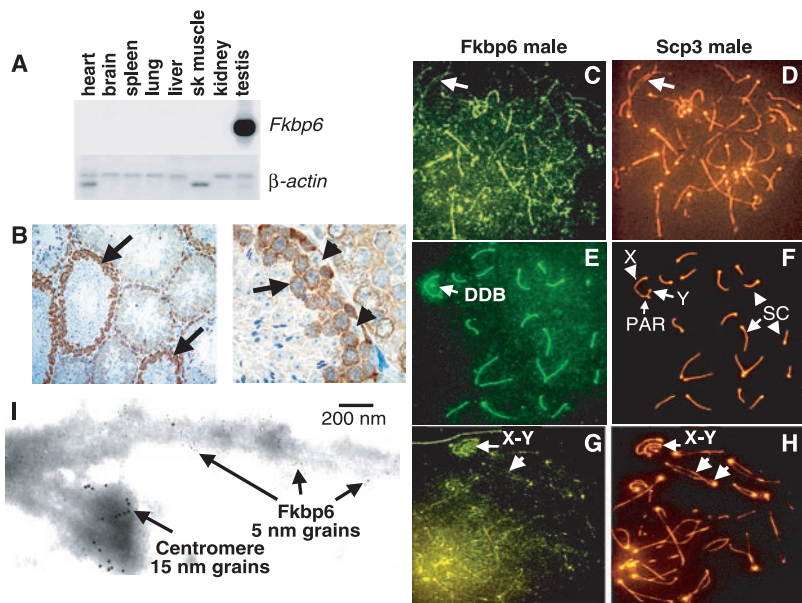


**Fig. 1.** (A) Murine *Fkbp6* mRNA expression.  $\beta$ -actin is shown as the control. Sk, skeletal. (B) Immunohistochemistry of *Fkbp6* in normal testis. Arrows show *Fkbp6* staining in meiotic spermatocytes. *Fkbp6* is absent in Sertoli cells (arrowheads). (C to H) Localization of *Fkbp6* and *Scp3* to the chromosome cores and SCs of mouse meiotic spermatocytes at the [(C) and (D)] zygote, [(E) and (F)] pachytene, and [(G) and (H)] diplotene stages. The pseudoautosomal regions (PAR), of the X and Y chromosomes are indicated. The male-specific DDB is shown. An anti-centromere antibody was used for counterstaining (orange). Arrows in (C) and (D) indicate the presence of *Fkbp6* on unpaired cores. Arrows in (G) and (H) show the X and Y chromosomes and chromosome separation in the diplotene stage. Analysis of meiotic chromosomes from *Fkbp6*<sup>-/-</sup> mice revealed that the *Fkbp6* antibody is specific (figs. S8 and S9). (I) Demonstration of *Fkbp6* as an SC protein in pachytene spermatocytes by EM with a 5-nm immunogold antibody to *Fkbp6*. The centromere is labeled with antiserum to CREST (15-nm grains).

tectable by Western blot (Fig. 3C) and immunohistochemistry (Fig. 3D). However, the genomic deletion of exon 8 did not result in an apparent alteration in *Fkbp6* mRNA expression (Fig. 3E). Whether the genomic deletion results in an unstable Fkbp6 protein and/or expression of a mutant Fkbp6 protein that lacks exon 8–encoded sequences needs to be determined. These data point to a critical role of the exon 8–encoded region in the stability and/or function of Fkbp6 in meiotic cells. Thus, a genomic deletion including exon 8 of the rat *Fkbp6* gene is causative for the aspermic phenotype in *as/as* rats.

Fkbp6 labels meiotic chromosome cores and, in males, the X chromosome–associated DDB (Fig. 1, C and E). Because loss of Fkbp6 in gene-targeted mice and deletion of *Fkbp6* exon 8 in *as/as* rats resulted in a defect in spermatogenesis, we examined the behavior of meiotic chromosome cores in *Fkbp6*<sup>-/-</sup> males. The assembly of chromosome cores and synapsis were similar at early prophase in *Fkbp6*<sup>-/-</sup> and control littermates. In *Fkbp6*<sup>-/-</sup> pachytene spermatocytes, there were multiple chromosome misalignments and nonhomologous partner switches of the chromosome cores, as demonstrated by fluorescence staining (Fig. 4A) and EM (Fig. 4, B and C). We frequently observed the presence of one or two X-chromosome loops, i.e., autosynapsed regions of the X-chromosome core (Fig. 4D). In meiotic nuclei of *Fkbp6*<sup>-/-</sup> cells, the numbers and localization of the Rad51/Dmc1 recombinase complexes appeared normal at the early stages of prophase (Fig. 4, E and F). *Fkbp6*<sup>-/-</sup> spermatocytes at later stages of meiosis that displayed chromosomal abnormalities showed massive accumulation of Rad51/Dmc1 expression at the chromosome cores (Fig. 4, E and F), suggesting large numbers of chromosome breaks in *Fkbp6*<sup>-/-</sup> spermatocytes. Cells in the later prophase stage of diplotene were completely absent in *Fkbp6*<sup>-/-</sup> testes (fig. S6). These synaptic abnormalities in the *Fkbp6*<sup>-/-</sup> spermatocytes show that Fkbp6 expression is required for the proper alignment and pairing of chromosome cores at meiotic prophase. Moreover, Fkbp6 may regulate progression and/or maintenance of chromosome synapsis.

It has been shown previously that in mutants that exhibit meiotic abnormalities, spermatogenesis frequently appears more severely compromised than oogenesis, suggesting sex-specific checkpoint differences (16). For instance, *Scp3* mutant males are infertile because of a block in spermatogenesis at the zygotene stage of meiosis, whereas loss of *Scp3* in females results in reduced fertility with reduced litter size and an increased likelihood of aneuploid progeny (6, 7). Because Fkbp6 is an SC protein in oocytes (fig. S2, E to H), we analyzed whether Fkbp6 has a role in fertility and meiosis in females. *Fkbp6*<sup>-/-</sup> females were able to breed up to 1 year after

birth, and individual *Fkbp6*<sup>-/-</sup> female mice carried multiple pregnancies with litter sizes comparable to those of control littermates. Histological analysis showed that ovaries and the differentiation of oocytes were comparable between *Fkbp6*<sup>-/-</sup> female and control littermates (fig. S7). Moreover, *Fkbp6*<sup>-/-</sup> oocytes progressed normally through all stages of meiosis and continued into late prophase and metaphase I. Alignment of chromosomes, chromosome pairing, Rad51/Dmc1 expression, and chromosome separation in meiotic oocytes of *Fkbp6*<sup>-/-</sup> females also appeared normal (Fig. 5, A and B). Male *as/as* rats are sterile, whereas females are fertile without any detectable abnormality (14).

Whether loss of Fkbp6 in females results in aneuploidy in the offspring needs to be studied. Our data indicate that loss of Fkbp6 has no apparent effect on meiotic chromosome pairing and fertility in females.

To elucidate a potential mechanism for Fkbp6 function, we speculated that Fkbp6 might bind to one of the known SC proteins. We immunoprecipitated Fkbp6 from primary spermatocytes and analyzed Fkbp6-associated proteins using matrix-assisted laser desorption/ionization–time-of-flight mass spectrometry (17). One of the associated proteins was identified as *Scp1*, and Fkbp6 and *Scp1* colocalized in autosomal chromosome synapsis in wild-type spermatocytes (fig. S2,

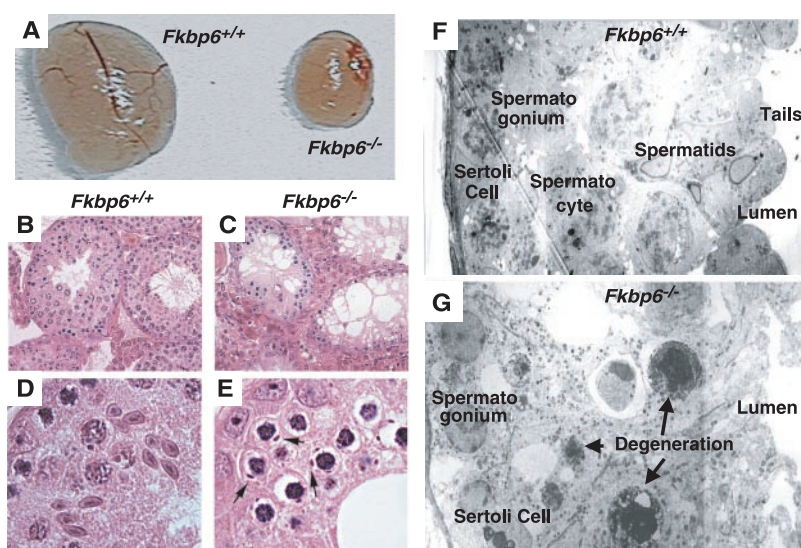


**Fig. 2.** Complete block in spermatogenesis in *Fkbp6*<sup>-/-</sup> mice. (A) Isolated testis from 16-week-old *Fkbp6*<sup>+/+</sup> and *Fkbp6*<sup>-/-</sup> mice. (B to E) Hematoxylin and eosin–stained testis sections from 16-week-old mice. [(B) and (D)] *Fkbp6*<sup>+/+</sup> mice. [(C) and (E)] *Fkbp6*<sup>-/-</sup> mice. Spermatids are completely absent and unique inclusion bodies are present in abnormal spermatocytes (arrows) in the testes of *Fkbp6*<sup>-/-</sup> mice. [(F) and (G)] EM cross sections of (F) an *Fkbp6*<sup>+/+</sup> seminiferous tubule, showing Sertoli cells, spermatogonia, pachytene spermatocytes, spermatids, and spermatozoa tails in the lumen; and (G) an *Fkbp6*<sup>-/-</sup> seminiferous tubule with defective germ-cell development. Multiple pachytene spermatocytes display cellular degeneration and there are no postpachytene nuclei. Spermatids and spermatozoa are completely absent.

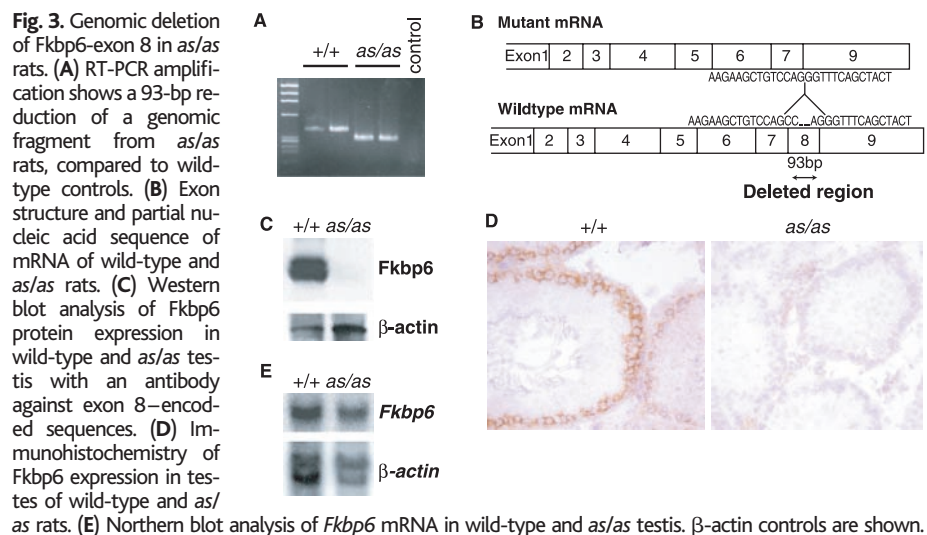


**Fig. 3.** Genomic deletion of *Fkbp6*-exon 8 in *as/as* rats. (A) RT-PCR amplification shows a 93-bp reduction of a genomic fragment from *as/as* rats, compared to wild-type controls. (B) Exon structure and partial nucleic acid sequence of mRNA of wild-type and *as/as* rats. (C) Western blot analysis of Fkbp6 protein expression in wild-type and *as/as* testes with an antibody against exon 8–encoded sequences. (D) Immunohistochemistry of Fkbp6 expression in testes of wild-type and *as/as* rats. (E) Northern blot analysis of *Fkbp6* mRNA in wild-type and *as/as* testes.  $\beta$ -actin controls are shown.

## REPORTS

A to D). In *Scp3*<sup>-/-</sup> spermatocytes, in which the axial cores are still intact and residual chromosome synapsis occurs in meiotic spermatocytes, Fkbp6 was expressed at the residual chromosome synapsis (Fig. 5, C and D). Fkbp6 expression was also found at the full SCs in *Scp3*<sup>-/-</sup> oocytes; Scp1 and Fkbp6 colocalized in these synapses (Fig. 5D). These results show that Fkbp6 associates biochemically with Scp1 in meiotic germ cells and that, even in the absence of Scp3 expression,

Fkbp6 colocalizes with Scp1 at the regions of residual chromosome synapses. Thus, Fkbp6 associates with Scp1 and might be able to facilitate chromosome synapsis in the absence of Scp3 expression.

Because chromosome cores initiate synapsis in the early meiotic prophase of *Fkbp6*<sup>-/-</sup> mice (18, 19), it is not likely that Fkbp6 functions in synapsis initiation. The synaptic abnormalities at later prophase in *Fkbp6*<sup>-/-</sup> mice indicate that Fkbp6 plays a

role in monitoring progression and/or maintaining homologous synapsis and that its failure to do so results in the autosynapsis of the X-chromosome core, core misalignment, and nonhomologous partner switches. In contrast, genetic inactivation of murine Scp3 results in defective chromosome synapsis and spermatogenic arrest at the zygotene stage (6), suggesting that Fkbp6 and Scp3 have different functions in chromosome synapsis in males. Fkbp6 associates with Scp1 and these two proteins colocalize at the sites of residual chromosome synapses that are present in *Scp3*<sup>-/-</sup> spermatocytes. The sex-specific differences in male and female fertility and meiosis (16) in both *Fkbp6*<sup>-/-</sup> and *Scp3*<sup>-/-</sup> mice could be explained by functional redundancy between these two SC components in oocytes. It also will be important to determine if Fkbp6 interacts with other members of the SC such as Scp3 or Scp2. Moreover, the phenotype of *Fkbp6*<sup>-/-</sup> males resembles *Hsp70-2*<sup>-</sup> (20) and *Cyclin A*<sup>-</sup> (21) null mice. In particular, the connection to the HSP70-2 protein needs to be explored, because other members of the Fkbp family have been shown to bind to heat shock proteins associated with steroid receptors (22). Fkbp6 could also be involved in the control of meiotic checkpoints at the pachytene stage (23).

An estimated 15% of couples worldwide remain childless because of infertility (24). Few genetic causes of infertility have been identified in humans. Given our data from mouse mutants and spontaneously mutant rats, it may be interesting to test whether mutations in *Fkbp6* account for idiopathic human infertility and whether some Williams-Beuren syndrome patients display infertility due to homozygous disruptions in the *Fkbp6* gene. Our genetic data reveal a function for Fkbp-family proteins in the control of meiosis and male-specific fertility. The identification of Fkbp6 as a critical molecule in homologous chromosome pairing in meiosis suggests that other Fkbp6-family proteins might have a role in the control of chromosome pairing and chromosome stability in mitosis and cancer.

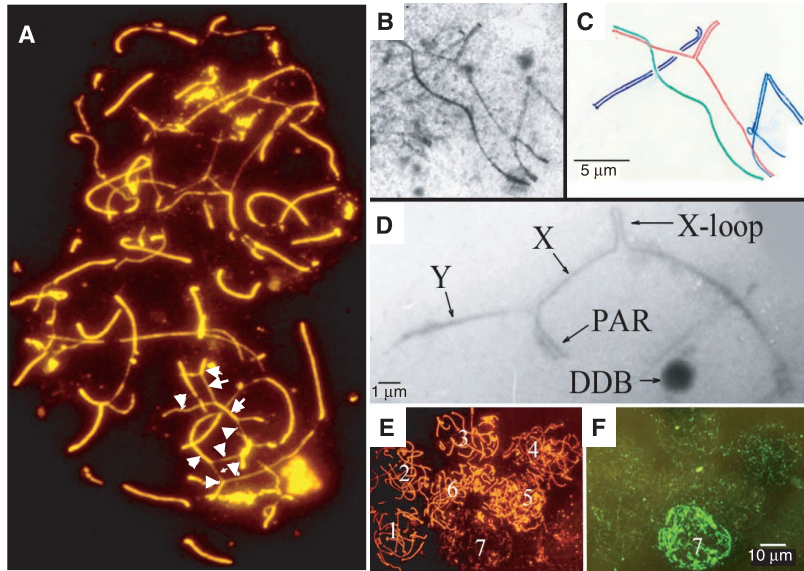
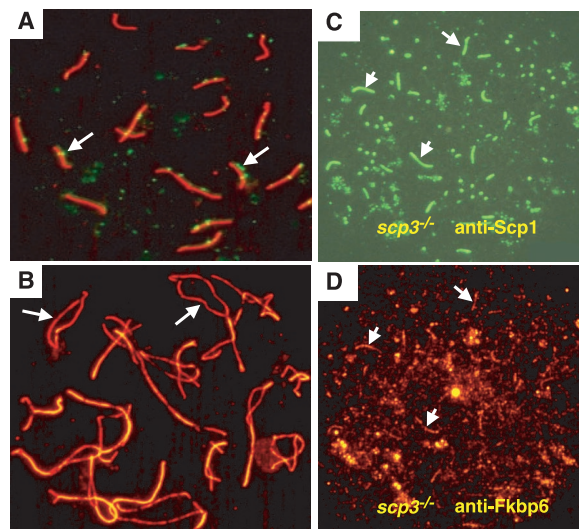


**Fig. 4.** Defective chromosome synapses in meiotic *Fkbp6*<sup>-/-</sup> spermatocytes. (A) Defective chromosome pairing in two *Fkbp6*<sup>-/-</sup> spermatocyte nuclei, stained with rhodamine-labeled antibodies to Scp3 (Scp3-rhodamine) and fluorescein isothiocyanate (FITC)-labeled antibodies to Scp1 (orange combined with red in the synapsed segments). Arrows mark partner exchanges and nonhomologous associations. (B) Electron micrograph of an *Fkbp6*<sup>-/-</sup> meiotic prophase nucleus. (C) Diagram of (B), illustrating multiple unpaired core segments and nonhomologous pairing between a red and a green core and between a red and a blue core in the *Fkbp6*<sup>-/-</sup> nucleus. (D) Electron micrograph of abnormal X-Y chromosome pairing and autosynapsis (an X-loop) in *Fkbp6*<sup>-/-</sup> prophase spermatocytes. (E) Seven spermatocyte nuclei in which the center lower nucleus is degenerating and losing Scp3 protein (rhodamine) expression. (F) The nuclei in (E) immunostained for Rad51/Dmc1 protein with FITC.

**Fig. 5.** Fkbp6 colocalizes with Scp1 in synapsed chromosomes of *Scp3*<sup>-/-</sup> spermatocytes. (A) Normal SC formation in pachytene oocytes stained with Scp3-rhodamine and FITC-labeled antibodies to Rad51 and Dmc1. Rad51 and Dmc1 foci (arrows) define regions of double-strand breaks. (B) Normal chromosome separation (arrows) in diplotene oocytes stained with Scp3-rhodamine, in a 1-day-old *Fkbp6*<sup>-/-</sup> female. (C and D) Expression of Fkbp6 and Scp1 in synapsed regions of *Scp3*<sup>-/-</sup> zygotene spermatocytes. (C) Short stretches of FITC-labeled Scp1 mark synapsis between the chromosome cores. (D) Fkbp6 (rhodamine) expression at the residual synapsed regions of *Scp3*<sup>-/-</sup> zygotene spermatocytes. Arrows in (C) and (D) show Scp1 and Fkbp6 colocalization.



## References and Notes

1. P. E. Cohen, J. W. Pollard, *Bioessays* **23**, 996 (2001).
2. K. Nasmyth, *Science* **297**, 559 (2002).
3. D. Zickler, N. Kleckner, *Annu. Rev. Genet.* **33**, 603 (1999).
4. D. W. Fawcett, *J. Biophys. Biochem. Cytol.* **2**, 403 (1956).
5. M. J. Moses, *J. Biophys. Biochem. Cytol.* **2**, 215 (1956).
6. L. Yuan *et al.*, *Mol. Cell* **5**, 73 (2000).
7. L. Yuan *et al.*, *Science* **296**, 1115 (2002).
8. X. Meng, X. Lu, C.A. Morris, M. T. Keating, *Genomics* **52**, 130 (1998).
9. L. R. Osborne, *Mol. Genet. Metab.* **67**, 1 (1999).
10. M. E. Dresser, M. J. Moses, *Chromosoma* **76**, 1 (1980).
11. M. F. Lyon, S. G. Hawkes, *Nature* **227**, 1217 (1970).
12. H. Ikadai, J. Noguchi, M. Yoshida, T. Imamichi, *J. Vet. Med. Sci.* **54**, 745 (1992).

13. Y. Atagi, H. Ikada, M. Kurohmaru, Y. Hayashi, *J. Vet. Med. Sci.* **55**, 301 (1993).
14. J. Noguchi *et al.*, *Mamm. Genome* **10**, 189 (1999).
15. M. Bayes *et al.*, *Mol. Reprod. Dev.* **60**, 414 (2001).
16. P. A. Hunt, T. J. Hassold, *Science* **296**, 2181 (2002).
17. Materials and methods are available as supporting material on Science Online.
18. P. B. Moens *et al.*, *J. Cell Sci.* **115**, 1611 (2002).
19. J. Y. Masson, S. C. West, *Trends Biochem. Sci.* **26**, 131 (2001).
20. D. J. Dix *et al.*, *Development* **124**, 4595 (1997).
21. D. Liu *et al.*, *Nature Genet.* **20**, 377 (1998).
22. P. K. Tai *et al.*, *Science* **256**, 1315 (1992).
23. T. Odorisio, T. A. Rodriguez, E. P. Evans, A. R. Clarke, P. S. Burgoyne, *Nature Genet.* **18**, 257 (1998).
24. M. M. Matzuk, D. J. Lamb, *Nature Cell Biol.* **4**, 41 (2002).
25. This study was partially funded by the Natural Sciences and Engineering Research Council of Canada and IMBA. J.M.P. holds a Canada Research Chair in Cell Biology. M.A.C. was supported in part by a Canadian Institutes of Health Research fellowship.

N.K.K. and P.E.C. are supported by AECOM. We would like to thank K. So for expert histology and C. Hoog for *Scp3<sup>-/-</sup>* mice.

#### Supporting Online Material

[www.sciencemag.org/cgi/content/full/300/5623/1291/DC1](http://www.sciencemag.org/cgi/content/full/300/5623/1291/DC1)

Materials and Methods  
Figs. S1 to S9

3 February 2003; accepted 25 April 2003

## Recruitment of HIV and Its Receptors to Dendritic Cell–T Cell Junctions

David McDonald,<sup>1</sup> Li Wu,<sup>2</sup> Stacy M. Bohks,<sup>3</sup>  
Vineet N. KewalRamani,<sup>2</sup> Derya Unutmaz,<sup>3</sup> Thomas J. Hope<sup>1\*</sup>

Monocyte-derived dendritic cells (MDDCs) can efficiently bind and transfer HIV infectivity without themselves becoming infected. Using live-cell microscopy, we found that HIV was recruited to sites of cell contact in MDDCs. Analysis of conjugates between MDDCs and T cells revealed that, in the absence of antigen-specific signaling, the HIV receptors CD4, CCR5, and CXCR4 on the T cell were recruited to the interface while the MDDCs concentrated HIV to the same region. We propose that contact between dendritic cells and T cells facilitates transmission of HIV by locally concentrating virus, receptor, and coreceptor during the formation of an infectious synapse.

Dendritic cells (DCs) comprise a multivariate family of cell types whose principal function is in the primary initiation of immune responses. Myeloid-derived dendritic cells (MDDCs) patrol areas of the body that are susceptible to invasion by pathogens and engulf antigens for later processing and presentation to T lymphocytes. The human immunodeficiency virus (HIV) has apparently appropriated this feature of the immune system to better establish and maintain infection of its primary target, CD4-positive T cells. HIV is taken up by MDDCs through interaction between its envelope glycoprotein, gp120, and mannose C-type lectin receptors (MCLR) expressed on the DC surface (1). The best characterized of these is DC-SIGN, a DC-specific C-type lectin (2). Rather than having the DC-HIV interaction lead to infection of the DCs, the bound HIV is efficiently transferred to target cells (2, 3). Further, HIV is internalized into a trypsin-resistant compartment, where its infectivity can be retained for an extended period of time before transfer (4).

<sup>1</sup>Department of Microbiology and Immunology, University of Illinois, Chicago, IL 60612, USA. <sup>2</sup>HIV Drug Resistance Program, National Cancer Institute at Frederick, Frederick, MD 21702, USA. <sup>3</sup>Department of Microbiology and Immunology, Vanderbilt University, Nashville, TN 37232, USA.

\*To whom correspondence should be addressed. E-mail: [thope@uic.edu](mailto:thope@uic.edu)

Dendritic cells are remarkably efficient at enhancing infection of targets. When we exposed cultured MDDCs to a CCR5-tropic HIV-1 vector encoding the firefly luciferase marker and then added appropriate targets, infectivity was enhanced significantly over a large range of input virus (Fig. 1A). We detected no luciferase activity when the Hut/CCR5 targets were not included, which indicated that the DCs did not become detectably infected under these conditions. To verify that the infectivity of CXCR4-tropic HIV that was tagged with green fluorescent protein (GFP) joined with HIV viral protein R (Vpr) (5) was also enhanced by MDDCs, we performed a similar experiment using  $\beta$ -galactosidase indicator cells (Fig. 1B). In addition to the enhancement seen under the coculture conditions, significant capture and transmission of infectious HIV was revealed by washing away unbound virus before challenging the target cells. All subsequent experiments used GFP-Vpr-labeled HIV, which allowed direct fluorescent imaging.

Cultured MDDCs are highly motile cells that tend to grow in suspension in vitro (6). After exposure to HIV, MDDCs bound varying amounts of virion particles, from a few to a few hundred per cell. Images of different focal planes of a representative MDDC showed that most of the HIV was found at or near the cell surface (Fig. 1, C and D; movie S1) (7).

We next asked whether the localization of HIV particles was altered when DCs contacted target cells. In a time-lapse experiment, two HIV-pulsed DCs were observed shortly after contact with adherent, CD4-positive cells (Fig. 2; movie S2). At the first time frame, the HIV was evenly distributed throughout both DCs. Within 6 min, the DC in the top of the frame began to spread out on the target, and the majority of the HIV relocated to the initial site of contact. Similarly, movement was observed in the other DC at 18 min. Although the HIV in the two DCs moved at different times, the majority of the particles moved within one 3-min time frame, which suggested rapid relocalization after cell-cell recognition.

To determine whether intracellular viral particles can also traffic to sites of cell contact, we performed time-lapse experiments on DCs that had been treated with protease after exposure to HIV. Much of the HIV signal remained after protease treatment, which suggested that these particles reside in an internal compartment not accessible to protease (4). When the HIV membranes were stained with a lipophilic dye during viral production (5), most of the GFP-labeled particles remained associated with the membrane dye even after trypsinization, which suggested that they were internalized as intact virions (8, 9). When the protease-treated DCs were immediately placed onto target cells, their adhesion to other cells was impaired. However, when the DCs were allowed to recover for an hour, adhesion was restored, and recruitment of the internalized viral particles occurred in a manner similar to that of DCs which had not been treated with protease (fig. S1, movie S2 to S5).

The recruitment of virus to sites of cell contact suggested a mechanism by which DCs might enhance viral infectivity. Antigen-presenting B cells interact with T cells to form a highly ordered, antigen-dependent junction known as the immunological synapse (10). Interactions between DCs and T cells are less well characterized. One apparent difference is that DCs are known to form antigen-independent structures with T cells. This interaction results in the recruitment of T cell receptor, CD4, and other molecules seen in the immunological synapse and induces low levels of signaling in the T cell but does not lead to activation (11). To determine